Manipulating topological quantum phase transitions of Kitaev's quantum spin liquids with electric fields

Pureum Noh [1,*] Kyusung Hwang [2,*] and Eun-Gook Moon [1,†]

[1]*Department of Physics, Korea Advanced Institute of Science and Technology (KAIST), Daejeon 34141, Korea*
[2]*School of Physics, Korea Institute for Advanced Study (KIAS), Seoul 02455, Korea*

Highly entangled excitations such as Majorana fermions of Kitaev quantum spin liquids have been proposed to be utilized for future quantum science and technology, and a deeper understanding of such excitations has been strongly desired. Here we demonstrate that Majorana fermion's mass and associated topological quantum phase transitions in the Kitaev quantum spin liquids may be manipulated by using electric fields in sharp contrast to the common belief that an insulator is inert under weak electric fields due to charge energy gaps. Using general symmetry analysis with perturbation and exact diagonalization, we uncover the universal phase diagrams with electric and magnetic fields. We also provide distinctive experimental signatures to identify Kitaev quantum spin liquids with electric fields, especially in connection with the candidate materials such as α-RuCl$_3$.

Introduction. Quantum spin liquids (QSLs) intrinsically host an enormous amount of quantum entanglement, which has attracted a great deal of interest in the research of future science and technology [1–5]. The intrinsic massive entanglement prevents quantum spin liquids from developing a trivial magnetic ordering, and instead emergent novel excitations may appear in QSLs. Kitaev quantum spin liquid (KQSL) is one of QSL that has attracted significant attention [6]. In KQSLs, the interactions between spin degrees of freedom are exactly solvable, leading to emergent Majorana fermions and Abelian or non-Abelian anyons. These exotic properties make KQSLs promising platforms for topological quantum computation [7,8].

The search for candidate materials that can exhibit KQSL has been a major challenge in the field of condensed matter physics. In recent years, significant progress has been made in identifying and characterizing KQSL candidate materials, such as α-RuCl$_3$ [9–18] and Na$_2$Co$_2$TeO$_6$ [19,20], through various experiments [21–24]. One of the unique features of KQSLs is their response to external magnetic fields, which can induce exotic phases such as a chiral spin liquid [6]. Despite the theoretical predictions, the experimental investigation of KQSLs in magnetic fields has remained challenging due to the need to explore a narrow range of magnetic field [12,24–37].

In this Letter, we demonstrate striking characteristics of electric-field-driven topological quantum phase transitions (TQPTs). First, varying with the amplitude of electric fields (E), we find TQPTs between critical states and bulk energy-gapped states. The former (latter) states host a Fermi surface of Majorana fermions, also called Majorana-Fermi surface (MFS) [38], (topological invariants) for $E < E_c^l$ ($E > E_c^l$). We

remark that the presence of such TQPTs is in drastic contrast to the conventional wisdom in the literature that the size of the Fermi surfaces of Majorana fermions is proportional to E. Second, by rotating an electric field, we find the possibility of the two types of TQPTs between the phases with opposite topological invariants. One type is conventional in the sense that TQPTs appear with quantum critical points, but the other type permits in-between quantum critical states. Remarkably, the two types of TQPTs are only possible for the intermediate amplitude of electric fields because they are washed away for small enough electric fields and KQSLs become unstable for strong enough electric fields. By utilizing the characteristics, we also propose how to detect KQSLs in the candidate materials such as α-RuCl$_3$.

Model Hamiltonian. Let us consider the isotropic Kitaev model under electric (**E**) and magnetic fields (**h**) to be specific and discuss its generalization below. The Hamiltonian is

$$H(\mathbf{h}, \mathbf{E}) = K \sum_{\langle i,j \rangle_\gamma} S_i^\gamma S_j^\gamma - \mathbf{h} \cdot \mathbf{S} - \mathbf{E} \cdot \mathbf{P}, \quad (1)$$

where $\langle i, j \rangle_\gamma$ are for the nearest-neighbor bonds with a component $\gamma \in \{x, y, z\}$, and S_j^γ is a γ component spin operator at a site j [6]. The total spin operator is defined as $\mathbf{S} = \sum_j \mathbf{S}_j$, and the interaction parameter (K) for the bond-dependent exchange interaction is introduced.

The explicit form of the electric polarization operator (**P**) may be obtained by microscopic analysis [39–41], and for our purposes, it is enough to utilize the symmetry approach, following the previous works [38,41]. Since **P** is even under the time-reversal transformation and odd under the space-inversion transformation, the polarization operator becomes $P^\mu \equiv \sum_{\langle i,j \rangle_\gamma} \mathbf{p}_\gamma^\mu \cdot (\mathbf{S}_i \times \mathbf{S}_j)$, where $\mathbf{p}_\gamma^\mu$ is a vector with 27 components. For the isotropic Kitaev model, only five ($c_1 \sim c_5$) of 27 parameters are independent [39–41],

$$\mathbf{p}_\alpha^\alpha = c_1 \hat{\alpha} + c_2(\hat{\beta} + \hat{\gamma}), \quad \mathbf{p}_\beta^\alpha = c_3 \hat{\alpha} + c_4 \hat{\beta} + c_5 \hat{\gamma},$$

*These authors contributed equally to this work.
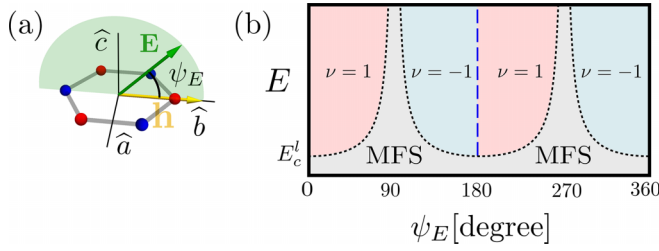
†egmoon@kaist.ac.kr

FIG. 1. The universal topological phase transition by electric fields. (a) Diagram of the direction of electric (**E**) and magnetic fields (**h**). The magnetic field is in the direction of $\hat{b}$, and the electric field lies in the $\hat{b} - \hat{c}$ plane. (b) The universal phase diagram at angles of the electric field (ψ_E) and the strength of the electric field (E) ranging from 0 to $|\mathbf{h}|$. The Chern number (ν) is not defined due to the Majorana-Fermi surface (MFS) in the gray area, and the lower critical strength E_c^l has the order of $\frac{|\mathbf{h}|^2}{\Delta_f}$. Dashed blue and dotted black lines indicate topological phase transitions.

where $c_1 \sim c_5$ are phenomenological coefficients, and (α, β, γ) is a permutation of (x, y, z).

Let us first consider the symmetries of the Hamiltonian. For an ideal monolayer system, the Hamiltonian $H(0, 0)$ enjoys $\mathbb{D}_3$, where $\mathbb{D}_3$ is for the dihedral group of order six, in addition to the spacial inversion ($\mathcal{P}$) and the time reversal ($\mathcal{T}$). Turning on a magnetic field, the time reversal and $\mathbb{D}_3$ symmetries are completely broken except in certain directions of the magnetic fields. For example, the Hamiltonian $H(\mathbf{h} \parallel \hat{\mathbf{b}}, 0)$ only enjoys the twofold rotational symmetry along $\hat{\mathbf{b}}$ and $\mathcal{P}$. See Fig. 1(a) for the notation of the directions of fields.

Physical quantities are characterized by representations of symmetry groups. For example, the thermal Hall conductivity (κ_{ab}) is odd under $\mathcal{T}$ and $C_2(\hat{\mathbf{b}})$, and it is even under $\mathcal{P}$ (Table I). It has been well understood that the twofold rotational symmetry [$C_2(\hat{\mathbf{b}})$] protects the gapless condition of Majorana fermions in Kitaev quantum spin liquids.

TABLE I. Symmetry properties of physical observables under the time-reversal ($\mathcal{T}$), inversion ($\mathcal{P}$) and the twofold rotation [$C_2(\hat{\mathbf{b}})$]. The thermal Hall coefficient (κ_{ab}), topological invariant (ν), and the mass function $m(\mathbf{h}, \mathbf{E})$ are in the same representation while the chemical potential function [$\mu(\mathbf{h}, \mathbf{E})$] is in a different representation. We also present the functions of electric and magnetic fields in the two representations. All the quantities are invariant under threefold rotations. See the SM for more detailed information.

Physical quantities	$\mathcal{T}$	$\mathcal{P}$	$C_2(\hat{\mathbf{b}})$	$\mathcal{P}C_2(\hat{\mathbf{b}})$
$\kappa_{ab}(\mathbf{h}, \mathbf{E})$	odd	even	odd	odd
ν	odd	even	odd	odd
$m(\mathbf{h}, \mathbf{E})$	odd	even	odd	odd
$h_x + h_y + h_z$	odd	even	odd	odd
$h_x h_y h_z$	odd	even	odd	odd
$E_c(E_a h_a + E_b h_b)$	odd	even	odd	odd
$h_a(E_a^2 - E_b^2) - 2h_b E_a E_b$	odd	even	odd	odd
$\mu(\mathbf{h}, \mathbf{E})$	odd	odd	odd	even
$h_a E_b - h_b E_a$	odd	odd	odd	even
$E_c h_b(h_b^2 - 3h_a^2)$	odd	odd	odd	even

Turning on an electric field, all the symmetries are completely broken except in two cases:

- $\mathbf{E} \parallel \hat{\mathbf{b}}$, $\mathbb{G}_b \equiv \{C_2(\hat{\mathbf{b}}), (C_2(\hat{\mathbf{b}}))^2\}$,
- $\mathbf{E} \parallel \hat{\mathbf{c}}$, $\mathbb{G}_c \equiv \{\mathcal{P}C_2(\hat{\mathbf{b}}), (\mathcal{P}C_2(\hat{\mathbf{b}}))^2\}$,

where $\mathbb{G}_{b,c}$ are the symmetry groups for each case. We note that the case of $\mathbf{E} \parallel \hat{\mathbf{c}}$ is not invariant under $C_2(\hat{\mathbf{b}})$ and $\mathcal{P}$ symmetries but invariant under the combination, $\mathcal{P}C_2(\hat{\mathbf{b}})$. Below, we show that both $\mathbb{G}_b$ and $\mathbb{G}_c$ protect the gapless Majorana fermions in KQSLs though their effects have significant differences in terms of TQPTs.

Weak electric and magnetic fields. Following the original approach of Kitaev [6], we utilize perturbative calculations with the Majorana representation of quantum spins ($S_j^\gamma = ic_j b_j^\gamma$) with four Majorana fermions (b_j^γ, c_j) at a site j for weak electric and magnetic fields ($|\mathbf{h}|, |\mathbf{E}| \ll K$). The low-energy effective Hamiltonian below the flux gap (Δ_f) becomes

$$H_{\text{eff}}(\mathbf{h}, \mathbf{E}) = \frac{1}{2} \sum_{\mathbf{k}} \Psi_{\mathbf{k}}^\dagger \left(\sum_{a=0,1,2,3} \epsilon_a(\mathbf{k}, \mathbf{h}, \mathbf{E}) \tau^a \right) \Psi_{\mathbf{k}},$$

with a two component spinor, $\Psi_{\mathbf{k}} = (c_{\mathbf{k},A}, c_{\mathbf{k},B})^T$, and $c_{\mathbf{r}, A(B)} = \sqrt{\frac{2}{N}} \sum_{\mathbf{k}} e^{i\mathbf{k}\cdot\mathbf{r}} c_{\mathbf{k}, A(B)}$. The identity and Pauli matrices in the sublattice spinor space ($\tau^{0,1,2,3}$) are introduced with the energy functions, $\epsilon_{0,1,2,3}(\mathbf{k}, \mathbf{h}, \mathbf{E})$. The eigenenergy of the Hamiltonian is

$$E_\pm(\mathbf{k}, \mathbf{h}, \mathbf{E}) = \epsilon_0(\mathbf{k}, \mathbf{h}, \mathbf{E}) \pm \sqrt{\sum_{a=1,2,3} \epsilon_a(\mathbf{k}, \mathbf{h}, \mathbf{E})^2}.$$

Without electric and magnetic fields, the energy functions vanish at the corners of the first Brillouin zone ($\mathbf{k} = \pm\mathbf{K}_M$), and the linear dispersion is determined by $\epsilon_1(\mathbf{k}, 0, 0)$ and $\epsilon_2(\mathbf{k}, 0, 0)$. As we turn on electric and magnetic fields, the Kitaev interaction (K) is renormalized by perturbation terms invariant under spatial inversion and time reversal, including E^2 terms as in previous papers [42–44] in the flux-free sector (see the Supplemental Material (SM) [45], also references [46–51] therein). We note that such symmetric terms can change our results quantitatively but not qualitatively because of symmetry properties of the topological invariant (ν). Thus, in the regime of weak electric and magnetic fields, the presence of energy gap or Fermi-surfaces of Majorana fermions is mainly determined by the chemical potential function [$\mu(\mathbf{h}, \mathbf{E}) \equiv \epsilon_0(\mathbf{K}_M, \mathbf{h}, \mathbf{E})$] and the mass function [$m(\mathbf{h}, \mathbf{E}) \equiv \epsilon_3(\mathbf{K}_M, \mathbf{h}, \mathbf{E})$]. If $|\mu(\mathbf{h}, \mathbf{E})| < |m(\mathbf{h}, \mathbf{E})|$, there is an energy gap, and the topological invariant (ν) is given by the sign of $m(\mathbf{h}, \mathbf{E})$. As for the case of $|\mu(\mathbf{h}, \mathbf{E})| > |m(\mathbf{h}, \mathbf{E})|$, the topological invariant is not defined because of the presence of MFS.

One can understand the symmetry properties of the energy functions by extending the original discussion of the projective representation by Kitaev [6] (see also the SM). Note that $m(\mathbf{h}, \mathbf{E})$ is in the same representation of κ_{ab}, while $\mu(\mathbf{h}, \mathbf{E})$ is in a different representation since it is odd under the inversion symmetry.

Our strategy is to utilize the symmetry properties of $m(\mathbf{E}, \mathbf{h})$ and $\mu(\mathbf{E}, \mathbf{h})$, which can be applied beyond the pure Kitaev model. For simplicity, we consider a magnetic field

along a bond direction and an electric field on the bc plane with an angle ψ_E,

$$\mathbf{h} = h\hat{\mathbf{b}}, \quad \mathbf{E} = E(\cos \psi_E \hat{\mathbf{b}} + \sin \psi_E \hat{\mathbf{c}}).$$

We find that

$$m(\mathbf{h}, \mathbf{E}) = c_m \frac{hE^2}{\Delta_f^2} \sin(2\psi_E), \quad \mu(\mathbf{h}, \mathbf{E}) = c_\mu \frac{h^3 E}{\Delta_f^3} \sin(\psi_E)$$

up to the fourth order of electric and magnetic fields with two dimensionless constants (c_m, c_μ). Note that the forms of $m(\mathbf{h}, \mathbf{E})$ and $\mu(\mathbf{h}, \mathbf{E})$ for generic field directions are presented in the SM.

A few remarks are as follows. First, the symmetry properties of the mass function [$m(\mathbf{E}, \mathbf{h})$] enforce the zero conditions,

$$m(\mathbf{h}, \mathbf{E}) = 0, \quad \mathbf{E} \parallel \hat{\mathbf{b}} \text{ or } \mathbf{E} \parallel \hat{\mathbf{c}}, \quad (2)$$

with magnetic fields along the bond directions, $\mathbf{h} \parallel \hat{\mathbf{b}}$. The zero conditions guarantee the existence of the gapless Majorana excitations. Second, the symmetry properties of the chemical potential function give the zero condition,

$$\mu(\mathbf{h}, \mathbf{E}) = 0, \quad \mathbf{E} \parallel \hat{\mathbf{b}}, \quad (3)$$

with magnetic fields along the bond directions, $\mathbf{h} \parallel \hat{\mathbf{b}}$. On the other hand, $\mu(\mathbf{h}, \mathbf{E})$ is not generically zero for $\mathbf{E} \parallel \hat{\mathbf{c}}$, which indicates that the Majorana Fermi surfaces may appear near $\mathbf{E} \parallel \hat{\mathbf{c}}$ because $|\mu(\mathbf{h}, \mathbf{E})|$ is generically bigger than $|m(\mathbf{h}, \mathbf{E})|$.

Two types of TQPTs. In KQSLs, we uncover the two types of TQPTs. The first one is conventional in the sense that topological phases with $\nu = \pm 1$ are generically connected through a quantum critical point, named type-I TQPT. In other words, gapless Majorana fermions appear only at quantum critical points. Not only the zero conditions [$m(\mathbf{h}, \mathbf{E}) = \mu(\mathbf{h}, \mathbf{E}) = 0$] but also the exclusion of Majorana Fermi surfaces are necessary to find such quantum critical points. The former is satisfied by $\mathbf{E} \parallel \hat{\mathbf{b}}$ and the latter is fulfilled by $|m(\mathbf{h}, \mathbf{E})| > |\mu(\mathbf{h}, \mathbf{E})|$ near $\mathbf{E} \parallel \hat{\mathbf{b}}$. Then, we obtain the condition of the type-I TQPTs,

$$\mathbf{E} \parallel \hat{\mathbf{b}}, \quad |\mathbf{E}| > E_c^l, \quad (\text{type I}), \quad (4)$$

where the lower critical electric field (E_c^l) is to exclude Majorana Fermi surfaces. Its value is determined by microscopic information. For example, the pure Kitaev model gives $E_c^l = (c_\mu h^2)/(2c_m \Delta_f)$, and the critical points are illustrated in the dashed blue line in in Fig. 1(b). The second one is unconventional in the sense that topological phases with $\nu = \pm 1$ are generically connected through quantum critical states with Majorana Fermi surfaces, named type-II TQPT. The transition lines are determined by the condition,

$$|m(\mathbf{h}, \mathbf{E})| = |\mu(\mathbf{h}, \mathbf{E})| > 0, \quad (\text{type II}), \quad (5)$$

as illustrated in the dotted black line in Fig. 1(b). We note that the type-II TQPT completely disappear with the fine-tuned condition, $c_\mu = 0$, for the pure Kitaev model. In other words, the presence of $\mu(\mathbf{h}, \mathbf{E})$ is essential to the presence of type-II TQPTs, and both the electric and magnetic fields are necessary, as pointed out previously [38].

Exact diagonalization. We diagnose the proposed quantum phase transitions by numerical computations for the spin
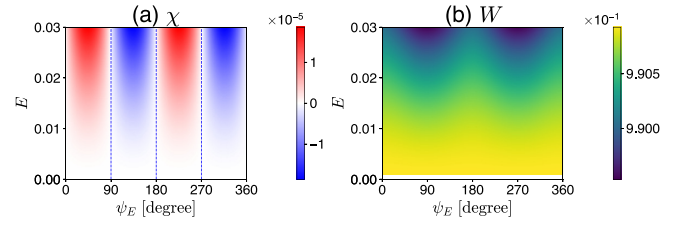

FIG. 2. Results of the exact diagonalization. (a) The expectation value of the chirality operator, χ. (b) The expectation value of the flux operator, W. The coupling constants are fixed by $K = -1$, $\mathbf{h} = 0.01\hat{\mathbf{b}}$, $\mathbf{E} = E(\cos \psi_E \hat{\mathbf{b}} + \sin \psi_E \hat{\mathbf{c}})$.

model in Eq. (1). For simplicity, we consider the model Hamiltonian,

$$H(\mathbf{h}, \mathbf{E}) = K \sum_{\langle i,j \rangle_\gamma} S_i^\gamma S_j^\gamma - \mathbf{h} \cdot \sum_j \mathbf{S}_j - \mathbf{E} \cdot \sum_{\langle i,j \rangle_\gamma} \mathbf{S}_i \times \mathbf{S}_j,$$

which is obtained by setting $c_1 = c_3$ and $c_{2,4,5} = 0$ in the polarization operator $\mathbf{P}$. We solve the Hamiltonian on a 24-site cluster with the periodic boundary condition by using exact diagonalization (ED).

Figure 2 displays the ED results for the same setup of Fig. 1. We identify a series of quantum phase transitions in our ED calculations, although the size limitation (24 sites) of our ED calculations prevents us from finding signatures of the Majorana fermi surface state. The identification is done by utilizing the symmetry properties of the chirality operator $\hat{\chi}_p$ following the previous work [32]: $\hat{\chi}_p = S_2^x S_1^z S_6^y + S_5^x S_4^z S_3^y + C_3$ rotated terms. Note that the chirality operator has the same symmetry representation as the one of thermal conductivity, providing information on the topological invariant of Kitaev quantum spin liquids. Indeed, the sign of the expectation value $\chi = \frac{1}{N} \sum_p \langle \hat{\chi}_p \rangle$ [Fig. 2(a)] appears in the same pattern as the Chern number of Fig. 1. We also note that the expectation value of the flux operator W is close to one ($W \approx 1$) in the range of the electric field ($|\mathbf{E}| \leqslant 0.03$), which indicates the stability of the Kitaev quantum spin liquids [Fig. 2(b)]. Thus, we conclude that our ED calculations qualitatively capture the topological phase transitions of Fig. 1 despite the intrinsic size limitation of our ED calculations.

It is straightforward to perform ED calculations for more generic Hamiltonians. For example, we find that the upper critical electric field is $E_c^u \approx 0.27$ without a magnetic field when $K = -1$ and $\mathbf{h}, \mathbf{E} \parallel \hat{\mathbf{c}}$, while the critical magnetic field is $h_c \approx 0.03$ without an electric field. Additional phase diagrams with magnetically ordered phases near KQSL are illustrated in the SM.

Based on the results of exact diagonalization, we conclude that the stability of the KQSLs under electric and magnetic fields is guaranteed, though their critical field values depend on details of the microscopic Hamiltonian. Then, the symmetry properties of Majorana fermions become very useful for stable KQSLs. Namely, the two zero conditions, Eqs. (2) and (3), are solely determined by the symmetry properties of $\mathbb{G}_{b,c}$, indicating that the zero conditions even work beyond the pure Kitaev model. It is straightforward to show that non-Kitaev interaction terms induce effective interaction between gapless Majorana fermions which are known to be irrelevant in the
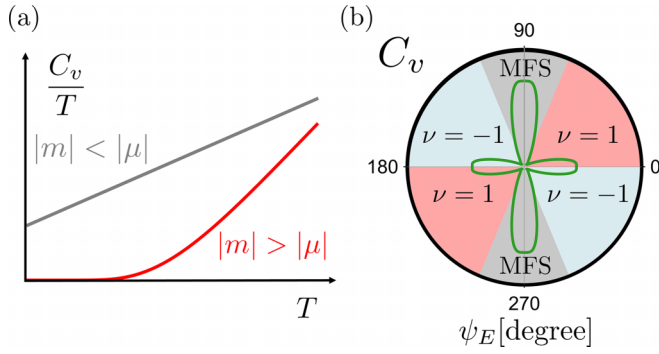
FIG. 3. Schematic low temperature specific heat (C_v) with magnetic fields and electric fields. (a) Temperature (T) dependence of $\frac{C_v}{T}$ with fixed electric and magnetic fields. (b) Angle dependence (ψ_E) of specific heat for $E > E_c^l$ with a fixed temperature.

sense of renormalization group analysis, in addition to trivial renormalization of velocity.

Discussion and conclusion. We propose that electric-field-driven TQPTs may be utilized to identify KQSLs. Varying with the amplitude of electric fields, TQPTs between critical states and bulk energy-gapped states generically appear. With $\mathbf{h} \parallel \hat{\mathbf{b}}$, a small electric field ($E < E_c^l$) cannot introduce an energy gap of Majorana fermions while a large electric field ($E_c^l < E < E_c^u$) induces a topological phase with a well-defined bulk energy gap. Such phase transitions may be readily observable in specific heat experiments, which carry low-energy excitations, as illustrated in Fig. 3(a). Furthermore, the rotation of an electric field is a natural way to observe the two types of TQPTs for $E_c^l < E < E_c^u$. We note that the type-II TQPTs around $\mathbf{E} \parallel \hat{\mathbf{c}}$ are natural outcomes of the zero conditions, Eqs. (2) and (3), which give a nonzero value of specific heat over temperature (C_v/T) in the zero temperature limit. Thus, the field angle dependence specific heat naturally has the twofold symmetric behavior as illustrated in Fig. 3(b). Such characteristics are in drastic contrast to other paramagnetic phases including partially polarized phases whose ground states are adiabatically connected to a simple product state without quantum entanglement [52].

To apply our proposal to experiments, it is important to obtain numerical values of E_c^l. For an easily accessible magnetic field (1T), we estimate $h \sim 0.12$ meV and then, for the typical

Kitaev exchange $|K| \sim 25$ meV [53], the corresponding lower critical strength of the electric field (E_c^l) and the energy scale are

$$E_c^l \sim 1.4 \times 10^6 \text{ V/m}, \quad c_3 E_c^l \sim 0.0049 \text{ meV} = 0.0002K,$$

where we utilize the previous estimation for $c_1 \sim c_5$ from the microscopic analysis [41] (see also the SM). Note that the critical electric field is indeed within the range of applicable electric fields, although our rough estimation needs to be scrutinized further to be applicable to the candidate materials of Kitaev quantum spin liquids such as α-RuCl$_3$.

We also note that the electric field smaller than E_c^l may give a nonzero value of C_v/T in the zero temperature limit as demonstrated in Fig. 3 except the direction $\mathbf{E} \parallel \hat{\mathbf{b}}$ where C_v/T vanishes in the zero temperature limit. Then, away from the direction $\mathbf{E} \parallel \hat{\mathbf{b}}$, the nonzero value and its angular dependence from the size of an MFS state will become more evidence of KQSLs.

In conclusion, we investigate the electric-field-driven TQPTs in KQSLs. In sharp contrast to the common belief that an insulator is inert under weak electric fields due to charge energy gaps, KQSLs may host significant effects with small electric fields because of nontrivial symmetry properties of Majorana fermions of KQSLs. We find TQPTs between critical states and bulk energy-gapped states varying with the amplitude of electric fields. Also, by rotating an electric field, we find the possibility of the two types of TQPTs between the phases with opposite topological invariants. Such TQPTs are associated with characteristic structures of gapless excitations, and thus we propose intriguing specific heat signatures in candidate materials of KQSLs such as α-RuCl$_3$.

[1] Y. Zhou, K. Kanoda, and T.-K. Ng, Quantum spin liquid states, Rev. Mod. Phys. **89**, 025003 (2017).

[2] L. Savary and L. Balents, Quantum spin liquids: A review, Rep. Prog. Phys. **80**, 016502 (2017).

[3] L. Balents, Spin liquids in frustrated magnets, Nature (London) **464**, 199 (2010).

[4] P. Anderson, Resonating valence bonds: A new kind of insulator? Mater. Res. Bull. **8**, 153 (1973).

[5] J. Knolle and R. Moessner, A field guide to spin liquids, Annu. Rev. Condens. Matter Phys. **10**, 451 (2019).

[6] A. Kitaev, Anyons in an exactly solved model and beyond, Ann. Phys. **321**, 2 (2006).

[7] C. Nayak, S. H. Simon, A. Stern, M. Freedman, and S. D. Sarma, Non-Abelian anyons and topological quantum computation, Rev. Mod. Phys. **80**, 1083 (2008).

[8] A. Kitaev, Fault-tolerant quantum computation by anyons, Ann. Phys. **303**, 2 (2003).

[9] K. W. Plumb, J. P. Clancy, L. J. Sandilands, V. V. Shankar, Y. F. Hu, K. S. Burch, H.-Y. Kee, and Y.-J. Kim, α − RuCl$_3$: A spin-orbit assisted Mott insulator on a honeycomb lattice, Phys. Rev. B **90**, 041112(R) (2014).

[10] A. Koitzsch, C. Habenicht, E. Müller, M. Knupfer, B. Büchner, H. C. Kandpal, J. van den Brink, D. Nowak, A. Isaeva, and T. Doert, J_{eff} description of the honeycomb Mott insulator $\alpha-RuCl_3$, Phys. Rev. Lett. **117**, 126403 (2016).

[11] L. J. Sandilands, Y. Tian, K. W. Plumb, Y.-J. Kim, and K. S. Burch, Scattering continuum and possible fractionalized excitations in $\alpha-RuCl_3$, Phys. Rev. Lett. **114**, 147201 (2015).

[12] H.-C. Jiang, Z.-C. Gu, X.-L. Qi, and S. Trebst, Possible proximity of the Mott insulating iridate Na_2IrO_3 to a topological phase: Phase diagram of the Heisenberg-Kitaev model in a magnetic field, Phys. Rev. B **83**, 245104 (2011).

[13] H.-S. Kim and H.-Y. Kee, Crystal structure and magnetism in $\alpha-RuCl_3$: An *ab initio* study, Phys. Rev. B **93**, 155143 (2016).

[14] S. M. Winter, A. A. Tsirlin, M. Daghofer, J. van den Brink, Y. Singh, P. Gegenwart, and R. Valentí, Models and materials for generalized Kitaev magnetism, J. Phys.: Condens. Matter **29**, 493002 (2017).

[15] S. M. Winter, Y. Li, H. O. Jeschke, and R. Valentí, Challenges in design of Kitaev materials: Magnetic interactions from competing energy scales, Phys. Rev. B **93**, 214431 (2016).

[16] S. M. Winter, K. Riedl, D. Kaib, R. Coldea, and R. Valentí, Probing $\alpha-RuCl_3$ beyond magnetic order: Effects of temperature and magnetic field, Phys. Rev. Lett. **120**, 077203 (2018).

[17] R. Yadav, N. A. Bogdanov, V. M. Katukuri, S. Nishimoto, J. van den Brink, and L. Hozoi, Kitaev exchange and field-induced quantum spin-liquid states in honeycomb α-RuCl$_3$, Sci. Rep. **6**, 37925 (2016).

[18] K. Imamura, S. Suetsugu, Y. Mizukami, Y. Yoshida, K. Hashimoto, K. Ohtsuka, Y. Kasahara, N. Kurita, H. Tanaka, P. Noh, J. Nasu, E.-G. Moon, Y. Matsuda, and T. Shibauchi, Majorana-fermion origin of the planar thermal Hall effect in the Kitaev magnet α-RuCl$_3$, Sci. Adv. **10**, eadk3539 (2024), .

[19] H. Takeda, J. Mai, M. Akazawa, K. Tamura, J. Yan, K. Moovendaran, K. Raju, R. Sankar, K.-Y. Choi, and M. Yamashita, Planar thermal Hall effects in the Kitaev spin liquid candidate $Na_2Co_2TeO_6$, Phys. Rev. Res. **4**, L042035 (2022).

[20] L. Viciu, Q. Huang, E. Morosan, H. Zandbergen, N. Greenbaum, T. McQueen, and R. Cava, Structure and basic magnetic properties of the honeycomb lattice compounds $Na_2Co_2TeO_6$ and $Na_3Co_2SbO_6$, J. Solid State Chem. **180**, 1060 (2007).

[21] M. Songvilay, J. Robert, S. Petit, J. A. Rodriguez-Rivera, W. D. Ratcliff, F. Damay, V. Balédent, M. Jiménez-Ruiz, P. Lejay, E. Pachoud, A. Hadj-Azzem, V. Simonet, and C. Stock, Kitaev interactions in the Co honeycomb antiferromagnets $Na_3Co_2SbO_6$ and $Na_2Co_2TeO_6$, Phys. Rev. B **102**, 224429 (2020).

[22] G. Lin, J. Jeong, C. Kim, Y. Wang, Q. Huang, T. Masuda, S. Asai, S. Itoh, G. Günther, M. Russina, Z. Lu, J. Sheng, L. Wang, J. Wang, G. Wang, Q. Ren, C. Xi, W. Tong, L. Ling, Z. Liu *et al.*, Field-induced quantum spin disordered state in spin-1/2 honeycomb magnet $Na_2Co_2Co_2TeO_6$, Nat. Commun. **12**, 5559 (2021).

[23] D. Wulferding, Y. Choi, S.-H. Do, C. H. Lee, P. Lemmens, C. Faugeras, Y. Gallais, and K.-Y. Choi, Magnon bound states versus anyonic Majorana excitations in the Kitaev honeycomb magnet α-RuCl$_3$, Nat. Commun. **11**, 1603 (2020).

[24] O. Tanaka, Y. Mizukami, R. Harasawa, K. Hashimoto, K. Hwang, N. Kurita, H. Tanaka, S. Fujimoto, Y. Matsuda, E. G. Moon, and T. Shibauchi, Thermodynamic evidence for a field-angle-dependent Majorana gap in a Kitaev spin liquid, Nat. Phys. **18**, 429 (2022).

[25] L. Janssen, E. C. Andrade, and M. Vojta, Honeycomb-lattice Heisenberg-Kitaev model in a magnetic field: Spin canting, metamagnetism, and vortex crystals, Phys. Rev. Lett. **117**, 277202 (2016).

[26] M. Gohlke, R. Moessner, and F. Pollmann, Dynamical and topological properties of the Kitaev model in a [111] magnetic field, Phys. Rev. B **98**, 014418 (2018).

[27] Z. Zhu, I. Kimchi, D. N. Sheng, and L. Fu, Robust non-Abelian spin liquid and a possible intermediate phase in the antiferromagnetic Kitaev model with magnetic field, Phys. Rev. B **97**, 241110(R) (2018).

[28] C. Hickey and S. Trebst, Emergence of a field-driven $U(1)$ spin liquid in the Kitaev honeycomb model, Nat. Commun. **10**, 530 (2019).

[29] J. Nasu, Y. Kato, Y. Kamiya, and Y. Motome, Successive Majorana topological transitions driven by a magnetic field in the Kitaev model, Phys. Rev. B **98**, 060416(R) (2018).

[30] S. Liang, M.-H. Jiang, W. Chen, J.-X. Li, and Q.-H. Wang, Intermediate gapless phase and topological phase transition of the Kitaev model in a uniform magnetic field, Phys. Rev. B **98**, 054433 (2018).

[31] J. Yoshitake, J. Nasu, Y. Kato, and Y. Motome, Majorana-magnon crossover by a magnetic field in the Kitaev model: Continuous-time quantum Monte Carlo study, Phys. Rev. B **101**, 100408(R) (2020).

[32] K. Hwang, A. Go, J. H. Seong, T. Shibauchi, and E.-G. Moon, Identification of a Kitaev quantum spin liquid by magnetic field angle dependence, Nat. Commun. **13**, 323 (2022).

[33] J. S. Gordon and H.-Y. Kee, Testing topological phase transitions in Kitaev materials under in-plane magnetic fields: Application to $\alpha-RuCl_3$, Phys. Rev. Res. **3**, 013179 (2021).

[34] D. C. Ronquillo, A. Vengal, and N. Trivedi, Signatures of magnetic-field-driven quantum phase transitions in the entanglement entropy and spin dynamics of the Kitaev honeycomb model, Phys. Rev. B **99**, 140413(R) (2019).

[35] A. Go, J. Jung, and E.-G. Moon, Vestiges of topological phase transitions in Kitaev quantum spin liquids, Phys. Rev. Lett. **122**, 147203 (2019).

[36] Y. Vinkler-Aviv and A. Rosch, Approximately quantized thermal Hall effect of chiral liquids coupled to phonons, Phys. Rev. X **8**, 031032 (2018).

[37] M. Ye, G. B. Halász, L. Savary, and L. Balents, Quantization of the thermal Hall conductivity at small Hall angles, Phys. Rev. Lett. **121**, 147201 (2018).

[38] R. Chari, R. Moessner, and J. G. Rau, Magnetoelectric generation of a Majorana-Fermi surface in Kitaev's honeycomb model, Phys. Rev. B **103**, 134444 (2021).

[39] S. Miyahara and N. Furukawa, Theory of antisymmetric spin-pair-dependent electric polarization in multiferroics, Phys. Rev. B **93**, 014445 (2016).

[40] A. Bolens, H. Katsura, M. Ogata, and S. Miyashita, Mechanism for subgap optical conductivity in honeycomb Kitaev materials, Phys. Rev. B **97**, 161108(R) (2018).

[41] A. Bolens, Theory of electronic magnetoelectric coupling in d^5 Mott insulators, Phys. Rev. B **98**, 125135 (2018).

[42] S. C. Furuya, K. Takasan, and M. Sato, Control of superexchange interactions with DC electric fields, Phys. Rev. Res. **3**, 033066 (2021).

[43] S. C. Furuya and M. Sato, Electric-field control of magnetic anisotropies: Applications to Kitaev spin liquids and topological spin textures, Phys. Rev. Res. **6**, 013228 (2024).

[44] D. J. Schultz, A. Khoury, F. Desrochers, O. Tavakol, E. Z. Zhang, and Y. B. Kim, Electric field control of a quantum spin liquid in weak Mott insulators, arXiv:2309.00037

[45] See Supplemental Material at http://link.aps.org/supplemental/10.1103/PhysRevB.109.L201105 for polarization operators, Majorana operator representation, symmetry properties, and additional results of exact diagonalization.

[46] I. A. Sergienko, C. Şen, and E. Dagotto, Ferroelectricity in the magnetic E-phase of orthorhombic perovskites, Phys. Rev. Lett. **97**, 227204 (2006).

[47] H. Katsura, N. Nagaosa, and A. V. Balatsky, Spin current and magnetoelectric effect in noncollinear magnets, Phys. Rev. Lett. **95**, 057205 (2005).

[48] M. Mostovoy, Ferroelectricity in spiral magnets, Phys. Rev. Lett. **96**, 067601 (2006).

[49] C. Jia, S. Onoda, N. Nagaosa, and J. H. Han, Bond electronic polarization induced by spin, Phys. Rev. B **74**, 224444 (2006).

[50] C. Jia, S. Onoda, N. Nagaosa, and J. H. Han, Microscopic theory of spin-polarization coupling in multiferroic transition metal oxides, Phys. Rev. B **76**, 144424 (2007).

[51] R. D. Johnson, S. C. Williams, A. A. Haghighirad, J. Singleton, V. Zapf, P. Manuel, I. I. Mazin, Y. Li, H. O. Jeschke, R. Valentí, and R. Coldea, Monoclinic crystal structure of $\alpha - RuCl_3$ and the zigzag antiferromagnetic ground state, Phys. Rev. B **92**, 235119 (2015).

[52] L. E. Chern, E. Z. Zhang, and Y. B. Kim, Sign structure of thermal Hall conductivity and topological magnons for in-plane field polarized Kitaev magnets, Phys. Rev. Lett. **126**, 147201 (2021).

[53] H. Li, H.-K. Zhang, J. Wang, H.-Q. Wu, Y. Gao, D.-W. Qu, Z.-X. Liu, S.-S. Gong, and W. Li, Identification of magnetic interactions and high-field quantum spin liquid in α-RuCl$_3$, Nat. Commun. **12**, 4007 (2021).